DESIGN OF A SMALL AXIAL-FLOW FAN WITH 0.2 HUB-TO-TIP RATIO

Massimo MASI[1], Andrea LAZZARETTO[2],
Piero DANIELI[1], Carlo BETTANINI[2]

[1] *University of Padova, Department of Management and Engineering, stradella S. Nicola 3, 36100 Vicenza, Italy*

[2] *University of Padova, Department of Industrial Engineering, via Venezia 1, 35121 Padova, Italy*

SUMMARY

This paper presents the design of a 315 mm axial fan obtained using the practical design approach recently proposed by the authors. Aim of the work is to explore the capability of the suggested method when a design with minimum hub-to-tip ratio is pursued. To this end, a 0.2 hub-to-tip ratio fan has been designed for the same dimensionless duty as an existing 1845 mm propeller fan, whose shape and performance are known from the literature. In the paper, the ISO 5801 aerodynamic performance are compared with those measured for the reference fan and its scaled model. The results demonstrate the effectiveness of the design approach and quantify the combined effect of size and Reynolds number on the fan performance.

INTRODUCTION

Industrial fans with hub-to-tip (ν) lower than 0.3 are widely applied both in small size (for example in the configuration closely coupled to finned heat exchangers for HVAC applications) and large size (for example in the air cooler condensers for large steam power plants). Many of these applications use the propeller-type fans, i.e. fans in which the casing limits to a minimum length duct (on the order of the axial length of the rotor) and a bell-mouth entry, when possible. Most of the effort in the design of these fans is devoted to the noise limitation. On the other hand, especially for very large units, aerodynamic performance and efficiency are of outmost importance. The subject of this paper is the aerodynamic design of a small propeller fan with $\nu = 0.2$. Although there are examples of large industrial fans with ν lower than 0.2, this value should be practically considered as the lower limit to place blade sections able to affect the fan aerodynamic performance. In fact, existing applications with $\nu < 0.2$ usually feature hub disk solution and non-

aerofoil profiles in the innermost part of the blade span that do not contribute to the fan aerodynamic performance [1].

Regarding the classic aerodynamic design methods, the scientific literature is still lacking in consolidated design methods for minimum ν propeller fans, although useful design guidelines for these units are available in classic fan design textbooks [2, 3]. Likely, the main reason of this lack is that the classical design theories rely on the cylindrical flow assumption without flow separation of the meridional current at the walls. This is a close approximation for the real flow as long as well-designed tube-axial or vane-axial fans (i.e. ducted fans with ν usually higher than 0.35) working at best efficiency operation are considered. However, this hypothesis loses its validity as the fan casing shortens and ν decreases, especially when the blade load departs from the free-vortex distribution and induces noticeable radial flow migration. Thus, computationally high demanding optimization techniques coupled with CFD (which also could account for noise issues) appear today as the only viable solution to improve the poor efficiency values credited by the literature [4] to minimum ν propeller fans designed according to empirical methods.

The present authors have recently suggested a practical design approach for tube-axial fans that allowed to achieve relatively high values of fan pressure and efficiency from 315mm prototypes with low ν [6]. According to this approach, the fans embed arbitrary vortex design rotors with approximately constant swirl at the rotor exit. The blade design process accounts for the radial flow migration to fix the proper staggering of each aerofoil section along the blade span. The method demonstrated no needs of CFD support to obtain aerodynamic performance comparable with those obtained from prototypes designed using more demanding optimisation techniques coupled with either CFD [7] or meta models derived from CFD [8]. However, the effectiveness of the design approach for ν noticeably lower than 0.3 is still worth to be investigated. To perform this investigation, experimental data from state-of-the-art propeller fans are necessary. For example, [9] reports the total-to-static pressure rise and efficiency curves measured for an 1845 mm propeller fan with $\nu = 0.14$, designed for cooling applications. Most important, the reference also includes almost all the fan geometrical data.

This paper presents the design of a propeller fan with 0.2 hub-to-tip ratio as obtained exploiting the practical design approach previously recalled and compares the aerodynamic performance of this design with those of the state-of-the-art 1845 mm propeller fan cited above. The aim of the paper is to assess the possible extension of the proposed design approach to the propeller-type fans with minimum ν. Since the results of the CFD simulations presented in [9] show that the reference fan blade induces an exit swirl resembling a rigid body rotation, it is expected that the design of the new fan will achieve a pressure rise noticeably lower than that of the reference fan. In fact, according to the design approach, the blades induce a constant swirl at the rotor exit that cannot exceed the minimum value for which hub separation occurs. Thus, it is worth investigating if:

i) the lower fan pressure is counteracted by a higher efficiency;
ii) there are means to increase the fan pressure without large penalty in the efficiency;
iii) the total-to-static maximum efficiency and the corresponding total-to-static fan pressure could be suited to propeller fan type applications.

The paper is organised as follows: the presentation of the reference fan and new fan design are followed by the description of the available instruments and tools, and the method used to assess by experiments the aerodynamic performance of the new design. The results report the comparison of the aerodynamic performance of the reference fan and new design. The latter is manufactured in two versions, one of which includes adjustments to improve the performance obtained by that resulting from the direct application of the practical design approach). Finally, the conclusions summarise the main advantages and drawbacks related to the extension of the practical design approach to minimum hub-to-tip ratio propeller fans.

REFERENCE FAN: GEOMETRY AND PERFORMANCE OF THE REF_FS FAN

The reference fan (REF_FS hereafter) is an 1845 mm propeller fan with $\nu = 0.14$. According to [9], REF_FS counts 6 rotor blades, positioned at ϕ_P (angle between the tip chord and the rotor mean plane) approximately equal to 15°. The aerofoil shaped part of the blade (i.e., the spanwise region at radial coordinate higher than 18 % of the fan diameter D) is obtained from envelope of Wortmann FX63-137 sections, untwisted in the outer blade part and staggered to obtain a blade twist equal to 4° in the innermost 75 % of the blade height. The total-to-static pressure rise and efficiency curves data have been rearranged in terms of fan pressure p_f, aeraulic efficiency η_{aer}, and total-to-static efficiency η_{TS} against fan flow rate q_v. Note that p_f, η_{aer}, and η_{TS} are defined in accordance with the ISO 5801 standard (fan pressure p_{fA}, fan total efficiency η_{fA}, fan static efficiency η_{fSA} respectively [5]). The orange crosses in Fig. 1 mark these data that are reported in dimensionless form as pressure coefficient $\Psi = p_f/(\omega D)^2$, flow rate coefficient $\Phi = q_v/(\omega D^3)$, aeraulic efficiency $\eta_{aer} = q_v\, p_f/(T\omega)$ and total-to-static efficiency $\eta_{TS} = q_v\, p_{fS}/(T\omega)$, where T and ω are the shaft torque and fan rotational speed, respectively.

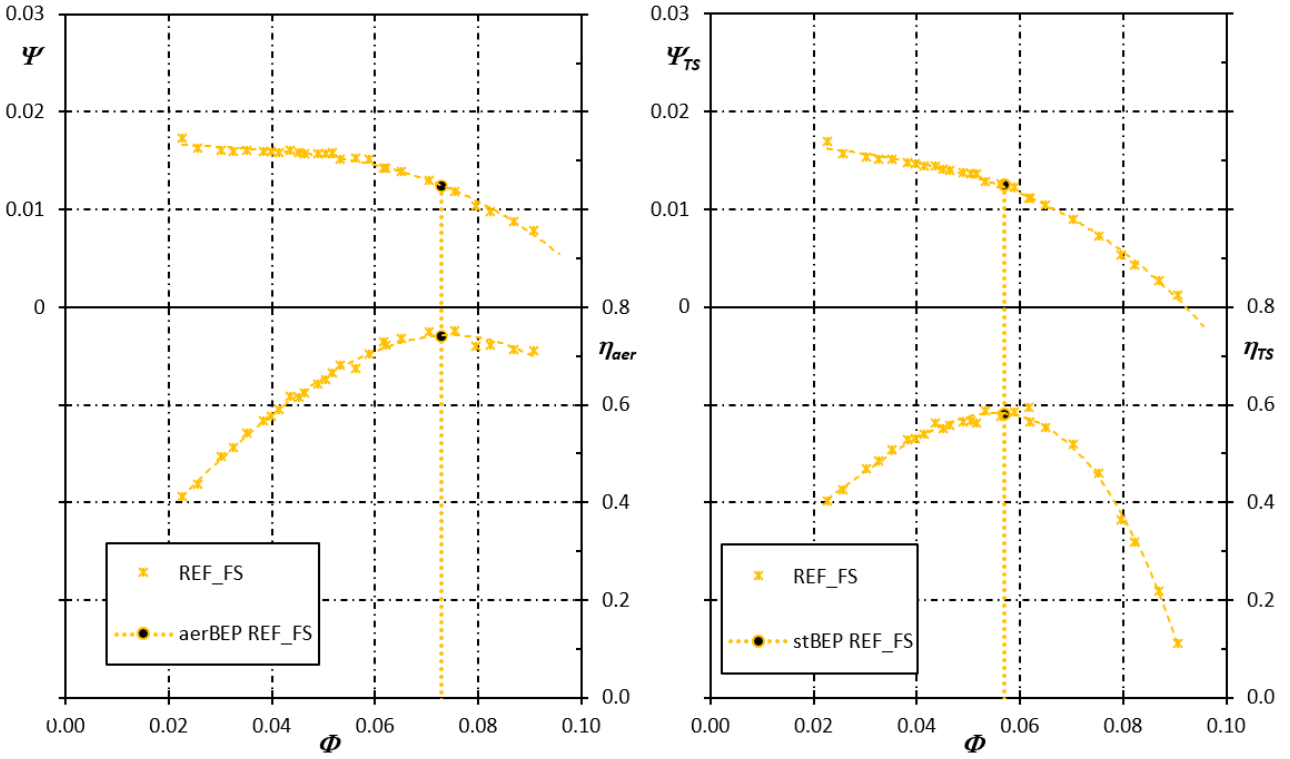

Figure 1: full scale data of the REF_FS fan (orange asterisk markers, adapted from [1]).
Filled circles mark the best efficiency operation.
Diagrams on the left and right side refer to the data with and without inclusion of the dynamic pressure.

NEW FAN: DESIGN OF THE 20R0B5 PROTOTYPE

According to Fig.1 data, the REF_FS best η_{aer} is approximately equal to 0.75 and it is obtained at $\Phi = 0.0728$, where the fan achieves $\Psi = 0.012$. Thus, $\Phi = 0.0728$ has been assumed as the design duty of the new fan. The design process relies on the practical approach suggested in [6] and therein described in detail. Accordingly, only the design steps are presented here and the reader is referred to [6] for the justification of each design step and the formulas used in this section. Note that the choice of assuming the best η_{aer} duty as design point instead of the best η_{TS} is fixed by the design approach that was originally conceived for tube-axial fans. It worth to mention that the new fan has

been designed with ν = 0.2, although REF_FS features ν = 0.14. This design choice should not affect the validity of the comparison because the CFD results reported in [1, 9] demonstrates that the non-aerofoil blade part (i.e. the part of the blade located below 18 % of the fan diameter) has negligible effect on REF_FS pressure and efficiency.

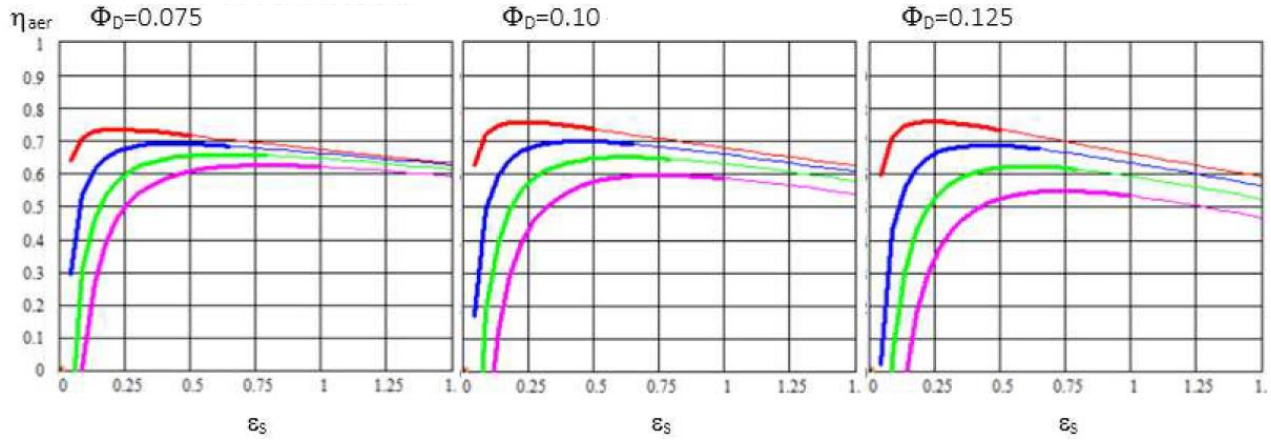

Figure 2: Tube-axial fan design charts of the aeraulic efficiency vs swirl coefficient for 3 values of the flow rate coefficient [10]. Red, blue, green, and magenta curves refer to hub-to-tip ratios equal to 0.2, 0.3, 0.4, and 0.5, respectively.

Figure 2 collects the values of η_{aer} achievable from well-designed tube-axial fans at three Φ_d operations, as predicted by the mean-line model developed in [10] for the fan preliminary design. The charts refer to the maximum efficiency operating condition of fans without tail-cone diffuser and with arbitrary vortex blading of the ε_S = const. type – being the swirl coefficient ε_S defined as the ratio between the swirl at the rotor exit and the mean axial velocity at the rotor entrance.

The new design started from the left side chart in Fig.2, valid for Φ_d = 0.075, i.e. a value very close to that chosen for the new fan. According to the red curve (ν = 0.2), a spanwise constant ε_S equal to 0.3 should result in a design that reaches $\eta_{aer} \approx$ 74 %.

The dimensionless mean radius x^* (which is representative of the entire blade aerodynamics) is equal to 0.66, in accordance with the following approximated relationship.

$$x^* = \begin{cases} \frac{1+\nu}{2} + \left[\sqrt{\frac{1+\nu^2}{2}} - \frac{1+\nu}{2}\right]\frac{\varepsilon_S}{0.6} & 0 \le \varepsilon_S < 0.6 \\ \sqrt{\frac{1+\nu^2}{2}} + \frac{1}{2}\left[\sqrt{\frac{1+\nu^2}{2}} - \frac{1+\nu}{2}\right]\frac{\varepsilon_S - 0.6}{0.6} & 0.6 \le \varepsilon_S < 1.6 \end{cases} \quad (1)$$

The parameters ν, Φ_d, x^*, and η_{aer} permit to conclude the preliminary design with the estimation of an expected fan pressure coefficient Ψ at design equal to 0.0071, using the following eq. (2).

$$\Psi = \frac{2}{\pi}\frac{x^*}{(1-\nu^2)}\Phi_d \varepsilon_S \eta_{aer} \quad (2)$$

This value is approximately 40 % lower than Ψ measured for the REF_FS fan at its best η_{aer} operation. As discussed in the Introduction, it was largely expected because of the lower blade load associated with the vortex design criterion adopted by the present design approach when applied with the constraint of no flow separation at the rotor hub.

The blade design process starts from the fulfilment of the radial equilibrium and the continuity equations at the rotor exit. A local value of the aerodynamic efficiency equal to 0.85 is assumed

along the entire blade span to obtain the dimensionless axial velocity ε_A (local to mean axial velocity ratio) at each radial position x of the rotor exit section. Equations (3) permit therefore to find the spanwise distribution of the mean relative flow angle β_m, and blade loading factor σC_L (neglecting the aerofoil drag).

$$\beta_m(x) = \operatorname{acos}\left(\frac{1}{2}\frac{1+\varepsilon_A(x)}{\sqrt{\frac{(1+\varepsilon_A(x))^2}{4}+\left(x\frac{\pi}{8}\frac{1-\nu^2}{\Phi_d}-\frac{\varepsilon_S}{2}\right)^2}}\right) \qquad \sigma C_L(x) = 2\frac{2\,\varepsilon_S}{(1+\varepsilon_A(x))}\cos[\beta_m(x)] \qquad (3)$$

A spanwise constant lift coefficient C_L equal to 0.7, and blade aspect ratio AR equal to 3.78 (i.e., blade height 3.78 times longer than chord at blade root), fix the spanwise distribution of the blade solidity σ and the rotor blade counts z (equal to 5). Note that, the practical design approach would have suggested σ at the hub not much lower than 1.2 (instead of 0.8 chosen here) and, accordingly, higher AR and/or z. The reason under the departure from the suggestion of the design approach is twofold: i), to obtain a design not very different from that of the REF_FS fan; ii), to permit in a second time the increase of z without unreasonable increase of σ.

The shape of the blade results from the envelope of 6 aerofoil sections staggered along a radial stacking line. The F-Series aerofoil section defined in Tab.1 has been used along the entire blade span. Chord length, and local incidence $\imath$ (equal to -5°), have been kept constant.

Table 1: main features of the selected F-series aerofoil section

Camber θ [°]	**Max. thickness [% of the chord]**	**C_L [-]**	**Attack angle [°]**
17.19	10	0.7	3

Each aerofoil has been placed in its own radial station x_n at an angle ϕ_P, obtained using eq. (5).

$$\phi_P(x_n) = \operatorname{atan}\left[\tan(\pi/2 - \xi(x_n))\ \cos(\Gamma)\right] \qquad (5)$$

where Γ is the obliquity of the meridional flow across the rotor blade passage and ξ is the stagger angle defined in accordance with eq. (6).

$$\xi(x_n) = \operatorname{atan}\left(\frac{x_n}{\frac{8}{\pi}\frac{\Phi_d}{1-\nu^2}}\right) - i - \theta/2 \qquad (6)$$

Note that, Γ was obtained by:

i) mass flow averaging the spanwise distribution of the obliquity derived from the solution of the radial equilibrium equation (26.6°);
ii) increasing the value so obtained up to 33°, to account for the limited constraint imposed to the radial flow migration by a dimensionless tip clearance approximately equal to 1.1 % of the blade height.

Hereafter this fan design is referred to as 20R0B5, where the first two digits stay for the hub size (in percentage of the casing diameter), R0 means that the blade staking line is radial with zero inclination of the aerofoil planforms with reference to the rotor axis (i.e. aerofoils placed onto cylindrical surfaces), and B5 indicates that the blades count is equal to 5.

INSTRUMENTS AND TOOLS

To minimise the modification to the experimental apparatus available in the Thermal and Aeraulic Machines Laboratory of the Department of Industrial Engineering at the University of Padova, each fan model considered in this paper features D equal to 315 mm and it has been manufactured in ABS by a rapid prototyping 3D printer. The aerodynamic performance has been measured on the available ISO5801 type-A test rig. The test rig manufacturing has been subject of a previous publication [11], whereas the original instruments included in the rig and their successive upgrade were described in [6] and [12], respectively. The measurements accuracy at best efficiency operation is not worse than 1.3 %, 1 %, and 2 % for q_v, p_f, and η_{aer} data, respectively. Figure 3 shows some pictures of the 3D printed models tested in this work, collected during the setup phase of the test campaign.

In this work the measurements system of the mechanical power has been upgraded to improve the accuracy of the overall measurement chain and in parallel achieve higher sampling frequency in the acquisition of experimental test points. To this end, the torque meter has been substituted with a high accuracy rotating slipring torque sensor model DR-1 by Lorenz Messtechnik® operating with rated accuracy class 0.1.

Conditioning for the torque meter's strain bridge is provided by a National Instruments® mod. 9219 Board, performing controlled voltage supply, analogue sampling at 100 Hz, 24-bit A/D conversion and data storage. Such relatively high-frequency acquisition allows to implement real time FFT of the torque signal identifying harmonic contributions linked to input rotations up to 3000 rpm. Accordingly, the rotational speed and the absorbed power data are immediately available, saving the additional time required to measure the shaft speed by the manual mechanical tachometer included in the previous measurement system.

The real-time monitoring of the fan shaft power also permits to verify the achievement of the steady-state operation of the test rig, preventing from considering data sets related to transient states.

Figure 3: 3D printed rotor of the 14REF model fan (left), 20REF and 20R0B5models mounted on the test rig (middle left and middle right), 20R0B10 model fan rotor (right).

ANALYSIS METHOD

The comparison of aerodynamic performance data in terms of similarity parameters is unavoidably affected by the differences in Reynolds number Re_c (based on blade chord and tip speed) and Size Parameter $SP = (p_f/\rho)^{0.25}/q_v^{0.5}$ [13], because the size and rotational speed of the REF_FS fan are noticeably different from those of the fans tested in the laboratory. Thus, it was decided to test a 3D printed model of the reference fan scaled down to 315 mm (14REF in Fig.3, and hereafter) and to compare its aerodynamic performance to that of the full-scale REF_FS fan. Moreover, to confirm by experiments that the increase of ν from 0.14 to 0.2 is negligible, as supposed in the design of the 20R0B5 prototype, also a modified version of the 14REF fan with ν increased to 0.2 (20REF in

Fig.3, and hereafter) has been printed and tested. The orange crosses and red triangles in Fig.3 mark the aerodynamic performance of 14REF and 20REF, respectively, in operation at the (Re_c, SP) pair equal to ($1x10^5$, 0.254 m). The data confirm the negligible effect of different ν values. In contrast, the comparison with the REF FS data at (Re_c, SP) approximately equal to ($5x10^5$, 1.238 m) shows that the 14REF and 20REF models suffer a strong decrease of η_{aer} and a shift of the best efficiency operation towards lower Φ. This was largely expected because of the remarkably lower values of Re_c [14]. In the present test campaign, also SP is deemed to be not negligible because:

i) the effect of different surface relative roughness is exacerbated by the poor surface finishing of the 3D printed material;
ii) it was not possible to replicate the REF_FS blade root in the 14REF model, because of the limited maximum tensile stress admitted by the model material;
iii) the small size of the 315 mm models makes difficult to obtain a precise alignment of rotor and casing axes and this impairs a rigorous control of the blade tip clearance.

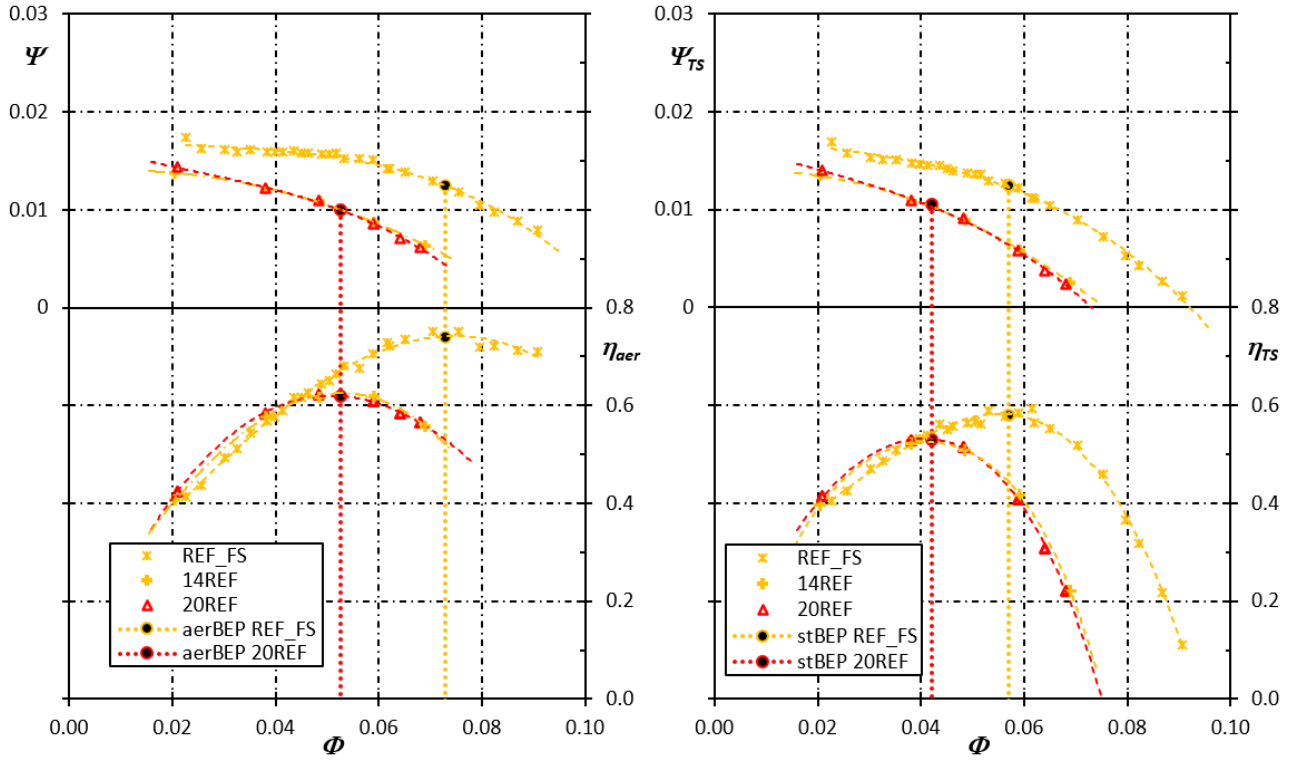

Figure 3: 14REF and 20REF models data (orange crosses and red tringles, respectively) and REF_FS data (orange stars). Best efficiency operations are marked by filled circles. Diagrams on the left and right side refer to the data with and without inclusion of the dynamic pressure.

Remarkably, experimental data also show a noticeable decrease of the 14REF and 20REF fan pressure if compared to the corresponding REF_FS data. This is compatible with the sensitivity of the Wortmann FX63-137 polar curve to Re_c. Unfortunately, due to mechanical constraints, it was not possible to test the 315mm fans operation at Re_c above $1x10^5$. Although several methods have been suggested in the literature to correct pressure and efficiency data accounting for the effect of Reynolds number (e.g. [15]), it was decided here to use a different strategy to compare the 20R0B5 prototype performance with those of the REF_FS fan. According to [2], the incorporation of some nose droop in the original aerofoil camberline allows to compensate the decrease of the pressure rise occurring at low-Re_c operation of fans designed using F-Series aerofoil sections, without much penalising the aerofoil efficiency. Thus, a nose droop equal to 3 % of the aerofoil chord has been added to the F-Series sections of the 315 mm 20R0 prototype, to "simulate" the performance achievable from the 20R0B5 design, if manufactured with the same size as the REF_FS fan. The nose droop was implemented in accordance with the instructions provided in [2].

RESULTS

Figure 4 superimposes the aerodynamic performance of the 20R0B5 prototype (black square markers) to the corresponding data of the REF_FS fan and 20REF model (orange markers already shown in Fig.3). As preliminary comment, note that the best η_{aer} operation of the R020B5 prototype matches almost perfectly the Ψ_d, although this Ψ value is obtained at Φ slightly lower than Φ_d. The inclusion of the aerofoil nose droop confirms to well compensates the Ψ decrease expected from the lower Re_c operation of the model. In fact, the magnitude of the best η_{aer} shift replicates that of corresponding data measured for two different 315mm tube-axial fans with higher ν [6] at comparable Re_c operations. Regarding the comparison with the REF_FS performance, the expected lack of Ψ is accompanied by trend and values of 20R0B5 η_{aer} that are noticeably better than those measured for the 20REF model at comparable Re_c and SP values. This finding is compatible with a possible improvement of the REF_FS efficiencies in case the R020B5 design is manufactured in the same size and operated at the same rotational speed as REF_FS fan.

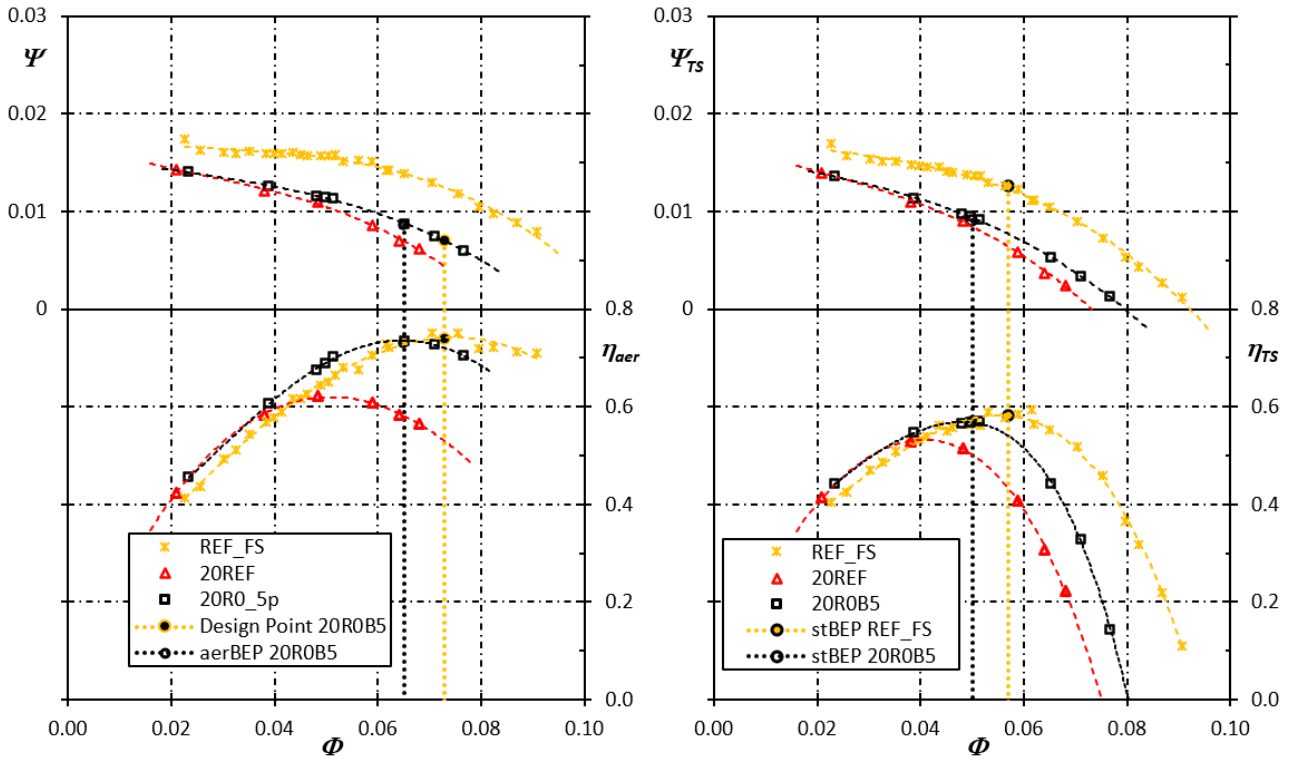

Figure 4: 20R0B5 model (black squares), 20REF model (red triangles) and REF_FS (orange crosses) data. Design point and effective best efficiency operations of the 20R0B5 prototype are marked by circles. Diagrams on the left and right side refer to the data with and without inclusion of the dynamic pressure.

Finally, the comparison between trends and values of the total-to-static performance curves measured for the two designs indicates that the 20R0B5 propeller fan design could be used in applications resembling those of the REF_FS, only if a lower total-to-static pressure rise at the same duty is acceptable. Thus, it is worth investigating if there are means to reduce the gap existing between the 20R0B5 design and the REF_FS fan Ψ curves, keeping a satisfactory efficiency level. There could be room for a performance increase by increasing the blade positioning angle. Alternatively, the performance can be increased without strong penalisation of efficiencies at design duty by increasing z at fixed AR (i.e., by increasing σ) noticing that:

i) the blade solidity chosen for the 20R0B5 is lower than that suggested by the practical design approach;
ii) the fan pressure scales with z in the isolated aerofoil assumption (which roughly holds for low-speed axial machines [4]).

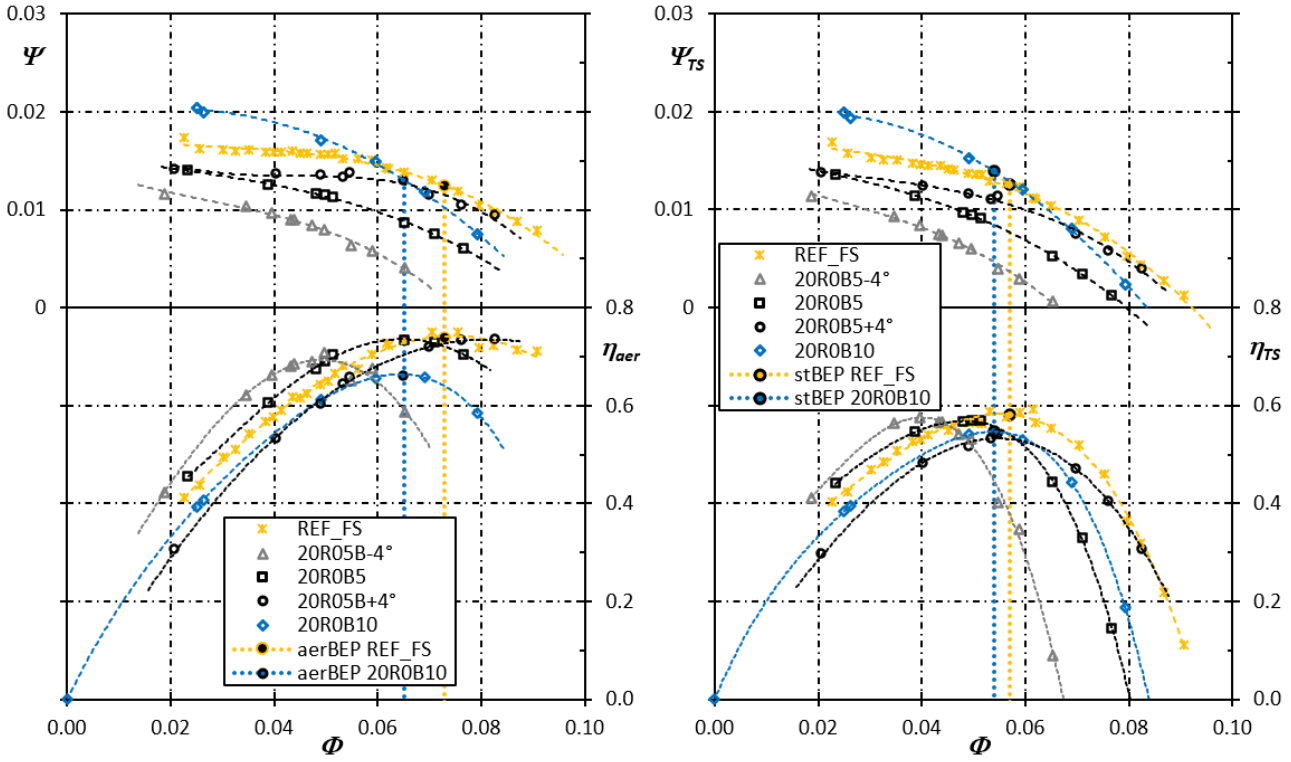

Figure 5: 20R0B10 model (blue diamonds), 20R0B5 model (black squares), 20R0B5 model with 4° blade positioning angle addition (black circles) and reduction (gray triangles), and REF_FS (orange crosses) data. Best efficiency point operations of the 20R0B10 prototype are REF_FS fan are marked by blue and orange circles, respectively. Diagrams on the left and right side refer to the data with and without inclusion of the dynamic pressure.

Figure 5 superimposes to the REF_FS and 20R0B5 data the aerodynamic performance curves measured for the 20R0B5 fan with 4° increase – named 20R0B5+4° – (and 4° reduction, 20R0B5-4°) of the blade positioning angle and 20R0B10 fan (i.e. the new fan design with z increased to 10). The improvement of the Ψ curve is apparent for the 20R0B5+4° and 20R0B10 fans: both the prototypes reach an aerodynamic performance not far from that of the REF_FS fan at best η_{aer} duty. Remarkably, the 20R0B5+4° best η_{aer} operation and 20R0B10 best η_{TS} operation almost match the corresponding operating conditions of the REF_FS fan.

CONCLUSIONS

The measured performance of the 0.2 hub-to-tip ratio propeller fan designed in accordance with the practical approach suggested by the authors demonstrated that this design method allows to match the design specifications also when applied to propeller fans with minimum hub-to-tip ratio The fan pressure at best efficiency duty is approximately 40 % lower than that achieved by a 1845 mm propeller fan with forced vortex-like blades, however the efficiency measured in small scale prototype tests is remarkably high and would exceed 75 % (i.e. the efficiency of the 1845 mm) in case of larger size and higher Reynolds number operation. In addition, it was demonstrated that the best aeraulic and total-to-static efficiency operating conditions of the 1845 mm fan can be almost matched by an increase of the blade positioning angle and blade counts, respectively, without strong efficiency penalisation. Moreover, the increase of blade counts allows for aerodynamic performance curves well suited to the original application of the 1845 mm fan.

ACKNOWLEDGMENTS

The authors gratefully acknowledge Gianfranco ZANON, who manufactured all the small mechanical components needed for the proper mounting of the models on the test rig, and Roberto LOSCO, who managed the rapid prototyping activity.

BIBLIOGRAPHY

[1] J. Wang, N. P. Kruyt – *Computational fluid dynamics simulations of aerodynamic performance of low-pressure axial fans with small hub-to-tip diameter ratio*. J. Fluids Eng., 142(9): 091202, **2020**

[2] R. A. Wallis – *Axial flow fans and ducts*. Reprint. Krieger Publishing, Malabar, **1993**

[3] B. Bruno – *Fans*. Pergamon Press. Oxford, UK, **1973**

[4] P. F. Bleier – *Fan handbook - Selection, application and design.* McGrawHill, New York. **1988**

[5] ISO 5810 – *Industrial fans – Performance testing using standardized airways*. **2007**

[6] M. Masi, A. Lazzaretto – *A new practical approach to the design of industrial axial fans: tube-axial fans with very low hub-to-tip ratio*. J. Eng. Gas Turbines Power, Vol. 141: pp. 101003-1/10, **2019**

[7] L. Yang, O. Hua, D. Zhao-Hui – *Optimization design and experimental study of low-pressure axial fan with forward-skewed blades*. Int. Journal of Rotating Machinery, Vol. 2007: Article ID 85275, **2007**

[8] K. Bamberger, T. Carolus – *Analysis of the flow field in optimized axial fans*. Proceedings of the ASME TurboExpo 2015. GT2015-43205. Montréal, Canada, **2015**

[9] J. Wang, N. P. Kruyt – *Validation of CFD simulations of aerodynamic performance of low speed axial fans with low hub-to-tip ratio*. Proceedings of AIAA SciTech Forum, Orlando, FL, **2020**

[10] M. Masi, S. Castegnaro, A. Lazzaretto – *A criterion for the preliminary design of high-efficiency tube-axial fans*. Proceedings of the ASME TurboExpo 2016. GT2016-56960. Seoul, South Korea, **2016**

[11] S. Castegnaro, M. Masi, A. Lazzaretto – *Design and testing of an ISO 5801 inlet chamber test rig and related issues with the Standard*. Proceedings of Fan 2018 Conference, Darmstadt, Germany, **2018**

[12] P. Danieli, M. Masi, G. Delibra, A. Corsini, A. Lazzaretto – *Assessment of MULTALL as computational fluid dynamics code for the analysis of tube-axial fans*. J. Turbomach., 143(7): 071005, **2021**

[13] M. Masi, L. Da Lio, A. Lazzaretto – *An insight into the similarity approach to predict the maximum efficiency of organic Rankine cycle turbines*. Energy, Vol. 198, 117278, **2020**

[14] Masi M., Castegnaro S., A. Lazzaretto – *Experimental investigation of the effect of Reynolds number on the efficiency of single-stage axial fans*. Proceedings ASME TurboExpo 2018. Oslo NOR, GT2018-76909. **2018**

[15] V. Casey, C. J. Robinson – *A unified correction method for Reynolds number, size, and roughness effects on the performance of compressors*. Proc. IMechE Part A: J. Power and Energy Vol. 225, pp.864-876, **2011**